

Stable Bounded Excursion Gravastars with Regular Black Holes

M. Sharif ^{*} and Faisal Javed [†]

Department of Mathematics, University of the Punjab,
Quaid-e-Azam Campus, Lahore-54590, Pakistan.

Abstract

This paper explores possible existence of stable regions of bounded excursion gravastars in the background of regular black holes (Bardeen and Bardeen-de Sitter black holes). For this purpose, we match internal de Sitter geometry with an external regular black hole through an intermediate shell with an equation of state. The matter surface located at the shell greatly affects the dynamical configuration of the shell. We consider stiff and dust fluids to discuss the outcomes of the developed structures. We then determine the critical values of physical parameters at which the shell neither collapses nor expands for both cases with different choices of external and internal geometries. It is found that there does not exist any possible region of stable bounded excursion gravastar for interior flat and exterior regular geometries. The stable bounded excursion gravastar is obtained for interior de Sitter and exterior regular black holes with a suitable choice of physical parameters for both stiff and dust shell. We conclude that possibility of the existence of both bounded excursion gravastars as well as black holes cannot be excluded in the dynamical model.

Keywords: Gravastars; Israel formalism; Stability analysis.

PACS: 04.70.Dy; 97.10.Cv; 04.40.Nr; 04.40.Dg

^{*}msharif.math@pu.edu.pk

[†]faisalrandawa@hotmail.com

1 Introduction

Gravitational collapse has been one of the interesting research fields which leads to the formation of different compact objects such as white dwarfs, neutron stars, naked singularities and black holes (BHs). In the light of theoretical and observational advances, there is often a set of paradoxical issues surrounding the BHs [1] that inspires scholars to try other solutions where massive stars are without horizons at their endpoints of gravitational collapse. Gravastars [2, 3], Bose superfluid [4] and black stars [5] are the few examples of such physical models. Within such simulations, gravastars have obtained special interest in recent times, in part owing to the strong relationship between the cosmological constant and the expanding universe [6], even though the presence of these stars may be limited very narrowly on observational grounds. A gravastar (gravitation expectation star) is an astronomic object which was proposed as an alternative of BH with no event horizon and singularity.

Mazur and Mottola [3] considered the Visser cut and paste approach to develop a gravastar model from the joining of exterior Schwarzschild BH with interior de Sitter (DS) spacetime. This model can be described in three different regions with the specific equation of state (EoS). The first region is denoted as an interior ($0 \leq r < r_1$), second is the intermediate ($r_1 < r < r_2$) and third is referred to as an exterior region ($r_2 < r$). In the first zone, a repulsive force is generated on the intermediate region by the isotropic pressure ($p = -\sigma$, where σ is the energy density). The intermediate region is assumed to be shielded by ultra-relativistic plasma and fluid pressure ($p = \sigma$). The exterior region is supported by the vacuum solution of the field equations with zero pressure ($p = 0 = \sigma$). This provides an effective thermodynamic solution with small fluctuations and maximum entropy.

The thin-shell matter surface produces an adequate amount of pressure to counteract the strength of gravity effects that maintain its configuration stable. Visser and Wiltshire [7] found the simplistic model to represent the Mazur-Mottola scenario by combining external and internal geometries using the cut and paste method. They evaluated the stable structure of gravastar with suitable choice of EoS for the transition layers. They also suggested that two separate forms of gravastars exist, i.e., stable and “bounded excursion” gravastars. Carter [8] extended this concept by the joining of interior DS spacetime and exterior Reissner-Nordström (RN) BH. They found stable configuration of the developed geometry for a wide range of physical pa-

rameters and also explored the respective qualitative characteristics of EoS. Horvat et al. [9] introduced theoretical electromagnetic gravastar model and investigated the effects of charge on stable gravastar configuration. The physical features such as entropy, proper length, and energy content of charged gravastar in (2+1)-dimensional spacetime was analyzed by Rahaman et al. [10].

Rocha and his collaborators [11] presented the prototype gravastar model by using external Schwarzschild BH and internal DS spacetime. They found that models sometimes represent stable “bounded excursion” gravastars, in which thin-shell oscillates between two final radii, otherwise, they collapse until BHs are formed. Hence, the possibility of the existence of a gravastar model cannot be excluded in such dynamical models. Chan et al. [12] proposed a dynamical model of prototype gravastars filled with phantom energy. It is found that the developed structure can be a BH, stable, unstable, or “bounded excursion” gravastar for various matter distributions at thin-shell. Later, this work was extended for the choice of exterior Schwarzschild-DS and RN spacetimes with interior DS region with specific EoS. They found that stable bounded excursion gravastar is obtained in the presence of exterior cosmological constant and charge [13, 14].

Lobo and Garattini [15] studied stability of noncommutative thin-shell gravastar and found that stable regions must be located near the predicted location of the event horizon. Övgün et al. [16] developed the gravastar model from the matching of external charged noncommutative BH with internal DS manifold. They noticed that the established framework satisfies the null energy condition and displays stable behavior for certain acceptable values of the physical parameter close to the predicted horizon. In the backgrounds of Bardeen/Bardeen-DS BHs, we have examined the stable regions of thin-shell gravastars through radial perturbation [17]. It is found that stable regions decrease for large values of charge and increase for higher values of the cosmological constant. There is a large body of literature [18]-[29] that explores the configuration of thin-shell constructed from the matching of various interior and exterior spacetimes.

The above-mentioned stable/unstable bounded excursion gravastar models are constructed in the background of exterior geometries with singularities. For the regular BHs (BHs without singularity), such geometrical structures have not been explored so far. Regular BHs are more interesting compact objects due to their regular center. Bardeen [30] was the pioneer to introduce a regular BH, an exact solution of the field equations that con-

tains an event horizon with a regular center. Afterward, some more models of regular BHs were proposed [31]. Bardeen BH can be used in DS and ADS backgrounds by Fernando [32]. There is a large body of literature that explored various characteristics of Bardeen-DS (ADS) BHs [33]-[38].

The current phase of our universe is accelerated expansion which has been verified through various observations [39]. A hypothetical form of energy with anti-gravitational effects is responsible to move apart all astronomical objects, referred to as dark energy. Its physical characteristics are different from the normal matter. To demonstrate the physical nature of dark energy, various models were proposed but the cosmological constant is the most suitable model to express the evolutionary behavior of the universe. By introducing the positive cosmological constant in the Einstein field equations, the corresponding spacetime has asymptotically positive curvature.

Regular BHs and the presence of cosmological constant motivate us to observe the geometrical structure and stable configuration of gravastars. Therefore, we consider Bardeen and Bardeen DS BHs to develop the geometrical structure of gravastars. This paper is devoted to present the formalism of a gravastar shell in the background of regular BHs through cut and paste technique. We explore the existence of stable bounded excursion gravastar for suitable values of physical parameters. The paper has the following format. Section 2 provides the construction of a gravastar shell and also evaluates the respective potential function by using the equation of motion with suitable EoS. In section 3, we investigate the developed structure for stiff and dust fluids in the presence of different exterior and interior geometries with critical values of physical parameters. Finally, we summarize our results in the last section.

2 Gravastar Model with Regular Black Holes

The line elements of lower and upper manifolds of gravastar shell in (3+1)-dimensions with coordinates (t, r, θ, ϕ) can be expressed as

$$ds^2 = g_{\mu\nu} dx^\mu dx^\nu = -k(1 - \lambda(r))dt^2 + (1 - \lambda(r))^{-1}dr^2 + r^2 d\Omega^2, \quad (1)$$

with the time coordinate scaling constant $k > 0$ and metric of unit 2-sphere is $d\Omega^2 = d\theta^2 + \sin^2 \theta d\phi^2$. Here, $\lambda(r)$ represents the compactness function

that can be written as

$$\lambda(r) = 2m(r)/r = 2/r \int_0^r 4\pi\bar{r}^2\sigma(\bar{r})d\bar{r}, \quad (2)$$

where $m(r)$ and $\sigma(r)$ denote the quasi-local mass function and energy density, respectively. The compactness function is directly related to the formation of event horizon in the considered spherically symmetric geometry. It is observed that the compactness function must be less than unity to avoid the existence of an event horizon. We consider the interior region of gravastar as DS manifold with cosmological constant Λ_i having constant energy density, i.e., $\sigma_i = \Lambda_i/8\pi \geq 0$. The respective compactness function of interior region is given as $\lambda_i(r) = 8\pi\sigma_i r^2/3 = r^2/L_i^2$ with $L_i = \sqrt{3/\Lambda_i}$, for $r < a(\tau)$ where $r = a(\tau) = a$ is the position of gravastar shell and τ denotes the proper time. It is noted that if $\lambda_i(r) \rightarrow 1$ then $r \rightarrow (3/\Lambda_i)^{1/2}$ which represents the position of DS/cosmological horizon.

Here, we use Bardeen DS manifold as exterior geometry with constant energy density as $\sigma_e = \Lambda_e/8\pi \geq 0$ so that the compactness function becomes [32]

$$\lambda_e(r) = 2mr^2/(r^2 + Q^2)^{3/2} + r^2/L_e^2, \quad r > a, \quad (3)$$

with $L_e = \sqrt{3/\Lambda_e}$, m is the mass of BH and Q represents the monopole charge of the geometry. This reduces to different manifolds for some specific values of physical parameters.

- If $\Lambda_e = 0$, $Q > 0$ and $M > 0$, then it denotes the Bardeen BH [30].
- If $\Lambda_e > 0$, $Q = 0$ and $M > 0$, it represents the Schwarzschild DS BH.
- If $\Lambda_e = 0 = Q$ and $M > 0$, then it corresponds the Schwarzschild BH.
- If $\Lambda_e > 0$ and $Q = 0 = M$, then it is clearly DS spacetime.

To avoid the event horizon in the gravastar geometry, the following conditions must be satisfied, i.e., (i) $\Lambda_i < 3/r^2$ for $r < a$, (ii) $\Lambda_e < 3/r^2 - 6m/(r^2 + Q^2)^{3/2}$ for $r > a$. These conditions indicate that Λ_i must be greater than Λ_e at $r = a$, i.e., $\Lambda_i > \Lambda_e$. This provides basic motivation behind the construction of the gravastar model that energy density of the surrounding region of the shell is less than the inner region.

The inner and outer regions are connected at the timelike hypersurface (Σ) , i.e., a (2+1)-dimensional spacetime, also referred to as a gravastar shell

with radius $r = a$. Such a matching is followed by the Visser's cut and paste procedure. This approach is useful to avoid the presence of event horizon as well as central singularity in the geometry of gravastars. We use Israel junction conditions to ensure that the developed structure is a solution of the field equations. These conditions are useful to evaluate the mass of the shell and potential function. The continuity of the line element (first junction condition) shows that the induced metric on Σ is identical for the metrics on both sides of Σ , i.e., $ds_i^2 = ds_e^2 = ds_\Sigma^2$ implying that $k_i(1 - \lambda_i(a)) = k_e(1 - \lambda_e(a))$. For the choice of Bardeen DS BH, $k_e \rightarrow 1$ and hence $k_i \rightarrow (1 - \lambda_e(a))/(1 - \lambda_i(a))$ that re-scales the time coordinate in the interior region.

The respective coordinates of Σ are denoted as $\xi^a = (\tau, \theta, \phi)$ and the line element (1) at $r = a$ becomes

$$ds^2 = [-(1 - \lambda(a)) + (1 - \lambda(a))^{-1}(da/d\tau)^2(d\tau/dt)^2] dt^2 + a^2 d\Omega^2. \quad (4)$$

The corresponding inducing metric at Σ is given as

$$ds_\Sigma^2 = h_{ab} d\xi^a d\xi^b = -d\tau^2 + a^2 d\Omega^2, \quad (5)$$

where $h_{ab} = g_{\mu\nu} e_a^\mu e_b^\nu$ is the induced metric tensor of Σ with $e_a^\mu = \partial x^\mu / \partial \xi^a$. By comparing Eqs.(4) and (5), we obtain

$$dt/d\tau = \dot{t} = \begin{cases} (1 - \lambda_i(a) + \dot{a}^2)^{1/2} / 1 - \lambda_i(a), & \text{for the interior region} \\ (1 - \lambda_e(a) + \dot{a}^2)^{1/2} / 1 - \lambda_e(a), & \text{for the exterior region} \end{cases} \quad (6)$$

The second condition leads to the continuity of extrinsic curvature (K_b^a) that shows smooth connection between inner and outer regions at Σ , i.e., $[K_b^a] = K_{b(i)}^a - K_{b(e)}^a = 0$. If $[K_b^a] = 0$, then it represents a boundary surface between these spacetimes, otherwise it leads to a thin-shell. The respective non-vanishing components of K_b^a at shell radius $r = a$ for Eq.(1) are given as

$$K_\tau^\tau = \begin{cases} (\lambda'_i(a) + 2\ddot{a}^2)/(1 - \lambda_i(a) + \dot{a}^2)^{1/2}, & \text{for interior region} \\ (\lambda'_e(a) + 2\ddot{a}^2)/(1 - \lambda_e(a) + \dot{a}^2)^{1/2}, & \text{for exterior region} \end{cases} \quad (7)$$

$$K_\theta^\theta = \begin{cases} (1 - \lambda_i(a) + \dot{a}^2)^{1/2}/a, & \text{for interior region} \\ (1 - \lambda_e(a) + \dot{a}^2)^{1/2}/a, & \text{for exterior region} \end{cases} \quad (8)$$

$$K_\phi^\phi = K_\theta^\theta \sin^2 \theta, \quad (9)$$

where $\lambda'(a)$ denotes differentiation of $\lambda(a)$ with respect to a . The matter surfaced at shell produces discontinuity in the extrinsic curvatures of both spacetimes. The standard expression of the stress-energy tensor for timelike hypersurface can be expressed as

$$S_b^a = -\frac{1}{8\pi}\{[K_b^a] - \delta_b^a K\}, \quad (10)$$

where $K = [K_a^a]$ and hence, we have [40]

$$- [K_\theta^\theta]/4\pi = (1 - \lambda_e(a) + \dot{a}^2)^{1/2}/4\pi a - (1 - \lambda_i(a) + \dot{a}^2)^{1/2}/4\pi a = \rho, \quad (11)$$

here $\rho = M/4\pi a^2$ is the energy density and M denotes the mass of gravastar shell. Using the values of compactness function of both spacetimes, the above equation can be written as

$$M + a \left[1 - \frac{2ma^2}{(a^2 + Q^2)^{3/2}} - \frac{a^2}{L_e^2} + \dot{a}^2 \right]^{1/2} - a \left[1 - \frac{a^2}{L_i^2} + \dot{a}^2 \right]^{1/2} = 0, \quad (12)$$

The effective potential of gravastar shell is followed from the equation

$$V(m, Q, M, L_i, L_e) + \dot{a}^2/2 = 0. \quad (13)$$

Now, we solve Eq.(12) for \dot{a}^2 to determine the mathematical expression of the effective potential as

$$\begin{aligned} V(a, m, Q, M, L_i, L_e) = & \frac{1}{2} - \frac{a^6}{8L_i^4 M^2} + \frac{ma^6}{2L_i^2 M^2 (Q^2 + a^2)^{3/2}} + \frac{a^6}{4L_i^2 M^2 L_e^2} \\ & - \frac{a^2}{4L_i^2} - \frac{a^6}{8M^2 L_e^4} - \frac{ma^6}{2M^2 L_e^2 (Q^2 + a^2)^{3/2}} - \frac{M^2}{8a^2} \\ & - \frac{m^2 a^6}{2M^2 (Q^2 + a^2)^3} - \frac{ma^2}{2(Q^2 + a^2)^{3/2}} - \frac{a^2}{4L_e^2}. \end{aligned} \quad (14)$$

We assume that the matter surface at gravastar shell follows the EoS [11]

$$p = (1 - \beta)\rho, \quad (15)$$

here p is the surface pressure and β is a constant. It is interesting to mention here that different values of β represent different types of matter distribution, i.e., standard energy ($\beta \leq 1.5$), dark energy ($1.5 < \beta \leq 2$) and phantom

energy ($\beta > 2$). The continuity of perfect fluid gives the relationship between the surface stresses of gravastar as

$$4\pi \frac{d}{d\tau}(a^2 \rho) + 4\pi p \frac{da^2}{d\tau} = 0, \quad (16)$$

which can be expressed as

$$\frac{d\rho}{da} = -\frac{2}{a}(\rho + p). \quad (17)$$

Using Eq.(15) and $\rho = M/4\pi a^2$ in (17), then solving, it follows that

$$M = ha^{2(\beta-1)}, \quad (18)$$

where h is an integrating constant.

The general expression of potential function is obtained by using Eq.(18) in (14) as

$$\begin{aligned} V(a, m, Q, L_i, L_e, h, \beta) &= \frac{a^{10-4\beta}}{4h^2 L_i^2 L_e^2} - \frac{a^{10-4\beta}}{8h^2 L_i^4} + \frac{ma^{10-4\beta}}{2h^2 L_i^2 (Q^2 + a^2)^{3/2}} - \frac{a^2}{4L_e^2} \\ &- \frac{m^2 a^{10-4\beta}}{2h^2 (Q^2 + a^2)^3} - \frac{ma^{10-4\beta}}{2h^2 L_e^2 (Q^2 + a^2)^{3/2}} - \frac{1}{8} h^2 a^{4\beta-6} \\ &- \frac{a^2}{4L_i^2} - \frac{ma^2}{2(Q^2 + a^2)^{3/2}} - \frac{a^{10-4\beta}}{8h^2 L_e^4} + \frac{1}{2}. \end{aligned} \quad (19)$$

To overcome the dependence of the potential function on the integration constant h , we redefine the physical parameters as follows

$$m \rightarrow mh^{\frac{1}{3-2\beta}}, \quad Q \rightarrow Qh^{\frac{1}{3-2\beta}}, \quad L_i \rightarrow L_i h^{\frac{1}{3-2\beta}}, \quad L_e \rightarrow L_e h^{\frac{1}{3-2\beta}}, \quad (20)$$

so that

$$\begin{aligned} V(a, m, Q, L_i, L_e, \beta) &= \frac{ma^{10-4\beta}}{2L_i^2 (Q^2 + a^2)^{3/2}} - \frac{m^2 a^{10-4\beta}}{2(Q^2 + a^2)^3} - \frac{ma^2}{2(Q^2 + a^2)^{3/2}} \\ &- \frac{ma^{10-4\beta}}{2L_e^2 (Q^2 + a^2)^{3/2}} - \frac{a^{10-4\beta}}{8L_i^4} + \frac{a^{10-4\beta}}{4L_i^2 L_e^2} - \frac{a^2}{4L_i^2} - \frac{a^2}{4L_e^2} \\ &- \frac{1}{8} a^{4\beta-6} - \frac{a^{10-4\beta}}{8L_e^4} + \frac{1}{2}. \end{aligned} \quad (21)$$

This is used to explore the expanding as well as collapsing characteristics of gravastar shell surrounded by the regular BH for suitable values of physical parameters m , Q , L_i , L_e and β .

3 Gravitational Collapse and Gravastars

This section explores the outcomes of the developed structure that can be a BH, stable/unstable or “bounded excursion” gravastar, or a Minkowski or DS geometry for various matter distributions at hypersurface. The potential function of the gravatar shell is used to characterize the final fate of the collapse through suitable physical parameters. The developed structure shows stable configuration against the radial perturbation for an equilibrium shell radius $a = a_0$, if

$$V(a_0) = 0, \quad V'(a_0) = 0, \quad V''(a_0) > 0. \quad (22)$$

At equilibrium shell’s radius, the shell’s motion along the radial direction vanishes, i.e., $\dot{a}_0 = 0 = \ddot{a}_0$. If $V''(a_0) < 0$, then it shows unstable behavior and it is unpredictable if $V''(a_0) = 0$. The stable bounded excursion is a less stringent concept to determine the stability of a geometrical structure. According to this notion, the shell’s motion must be bounded in between an interval (a_1, a_2) with $a_1 < a_2$ and follows the conditions

$$V(a_1) = 0, \quad V'(a_1) \leq 0, \quad V(a_2) = 0, \quad V'(a_2) \geq 0, \quad (23)$$

with $V(a) < 0, \forall a \in (a_1, a_2)$.

We use this approach to discuss the outcomes of the geometrical structure by using potential function and its derivative with respect to the shell radius. For this purpose, we solve simultaneously the following equations $V(m_c, Q_c, L_{ic}, L_{ec}, a_c) = 0 = V'(m_c, Q_c, L_{ic}, L_{ec}, a_c)$ and evaluate the respective critical values of the physical parameters like m_c , Q_c , L_{ic} , L_{ec} and a_c . The critical value of the shell radius (a_c) demonstrates the position of the shell at which it has neither expanding nor collapsing nature. These points of the geometrical structure can also be referred to as the saddle points. Similarly, the remaining critical values of the physical parameters also explain the position of the shell at saddle points. Due to complicated nature of Eq.(21), we cannot manipulate it analytically and hence consider some special cases. The specific values of physical parameters lead to different interior and exterior geometries of the shell. We do not consider the case $m = \Lambda_i = \Lambda_e = 0$ as it corresponds to the Minkowski spacetime in both interior as well as exterior regions and hence thin-shell disappears. Following special cases recover the previous results [11, 13, 14].

- $m = 0 = \Lambda_e$ and $\Lambda_i \neq 0$.

- $m = 0 = \Lambda_i$ and $\Lambda_e \neq 0$.
- $m \neq 0$, $Q = 0$ and $\Lambda_i = 0 = \Lambda_e$.
- $m \neq 0$, $Q = 0$ and $\Lambda_i \neq 0 \neq \Lambda_e$.

Here, we consider the following cases

- $m \neq 0 \neq Q$ and $\Lambda_i = 0 = \Lambda_e$.
- $m \neq 0 \neq Q$, $\Lambda_i \neq 0$ and $\Lambda_e = 0$.
- $m \neq 0 \neq Q$ and $\Lambda_i \neq 0 \neq \Lambda_e$.

In the following, we explore a suitable case for the construction of bounded excursion gravastar through effective potential with two different choices of matter distribution at the shell, i.e., stiff ($\beta = 0$) and dust ($\beta = 1$) fluids.

3.1 Stiff Fluid Shell

Here, we assume that the shell of the constructed model is filled with stiff fluid and the effective potential for such a matter distribution can be obtained by using $\beta = 0$ in Eq.(21). The corresponding expressions of the potential function and its derivative with respect to a are given as

$$\begin{aligned}
V(a) = & \frac{1}{2} + \frac{a^{10}}{4L_e^2 L_i^2} - \frac{a^{10}}{8L_e^4} - \frac{a^{10}}{8L_i^4} - \frac{1}{8a^6} - \frac{a^2}{4L_e^2} - \frac{a^2 m}{2(a^2 + Q^2)^{3/2}} - \frac{a^2}{4L_i^2} \\
& - \frac{a^{10} m}{2(a^2 + Q^2)^{3/2} L_e^2} + \frac{a^{10} m}{2(a^2 + Q^2)^{3/2} L_i^2} - \frac{a^{10} m^2}{2(a^2 + Q^2)^3}, \quad (24)
\end{aligned}$$

$$\begin{aligned}
V'(a) = & \frac{5a^9}{2L_e^2 L_i^2} - \frac{5a^9}{4L_e^4} - \frac{am}{(a^2 + Q^2)^{3/2}} + \frac{3a^{11}m}{2(a^2 + Q^2)^{5/2} L_e^2} - \frac{5a^9}{4L_i^4} - \frac{a}{2L_i^2} \\
& + \frac{3}{4a^7} - \frac{3a^{11}m}{2(a^2 + Q^2)^{5/2} L_i^2} + \frac{3a^{11}m^2}{(a^2 + Q^2)^4} - \frac{5a^9 m}{(a^2 + Q^2)^{3/2} L_e^2} \\
& + \frac{5a^9 m}{(a^2 + Q^2)^{3/2} L_i^2} - \frac{5a^9 m^2}{(a^2 + Q^2)^3} - \frac{a}{2L_e^2} + \frac{3a^3 m}{2(a^2 + Q^2)^{5/2}}, \quad (25)
\end{aligned}$$

respectively. These are used to discuss the dynamical configuration of a shell with suitable values of the physical parameters. We solve simultaneously $V(a) = 0$ and $V'(a) = 0$ for suitable values of Q . The solutions of this

system are used to determine the shell's radius at which the shell neither collapses nor expands. These values are also referred to as critical values of the physical parameters. We have obtained the respective critical values of physical parameters like a_c , Q_c , m_c , L_{ic} and L_{ec} for stiff matter distribution at the constructed shell as shown in Table 1. This table also explains the final outcomes of the developed structure with different choices of interior and exterior geometries. We explore the graphical behavior of the potential function corresponding to critical values of physical parameters. Here, we use three different possibilities to explore stable configuration of the developed structure with respect to the critical values, i.e., $m_1 < m_c < m_2$, $Q_1 < Q_c < Q_2$, $L_{i1} < L_{ic} < L_{i2}$ and $L_{e1} < L_{ec} < L_{e2}$. To obtain suitable results, we compare the graphical behavior through these choices, i.e., the system behavior for critical values and other values which are greater or smaller than critical values. For this purpose, we assume suitable values of the physical parameters close to the critical ones.

Case (i): $m \neq 0 \neq Q$ and $\Lambda_i = 0 = \Lambda_e$

This case denotes the internal flat region with external Bardeen BH and the respective critical values of physical parameters are shown in Table 1. For these values, the potential function shows neither expansion nor collapse at $a = a_c$ as shown in Figures 1-3. It is found that the effective potential approaches to $-\infty$ as $a \rightarrow \infty$ or 0. Thus the strictly negative behavior of potential function shows the formation of BH as an outcome of the gravitational collapse of a star. We also analyze the effects of mass and charge on the dynamical configuration of the star. Here, we obtain the results for different choices of mass and charge by considering $m < m_c$, $m = m_c$, $m > m_c$ and $Q < Q_c$, $Q = Q_c$, $Q > Q_c$ as shown in the left and right plots of Figures 1-3, respectively.

For $m < m_c$, the potential function has two real roots say a_1 and a_2 with $a_1 < a_2$. It is found that $V(a) < 0$ for $a < a_1$, $V(a) > 0$ for $a_2 < a < a_1$ and $V(a) < 0$ for $a > a_2$. This represents the unstable structure under small perturbation which leads to star either collapses until $a = 0$ and leaves behind a Bardeen BH or expands forever to form a flat spacetime (left plot of Figure 1). For $m = m_c$, the star shows collapsing behavior for $a < a_c$ until $a \rightarrow 0$ that leads to Minkowski spacetime and stops collapse or expansion at $a = a_c$ and then collapses continuously for $a > a_c$. The potential function is strictly negative for $m > m_c$ which corresponds to the formation of BH as

Table 1: Critical values of physical parameters and final outcomes of the developed structure for a stiff fluid shell with different choices of internal and external geometries. Here, we use the internal region (IR), external region (ER), structure (St), figures (Fig.) flat region (FR), Bardeen BH (B), Bardeen-DS BH (BDS), the normal star (NS) and gravastar (GS).

Final outcomes of the developed structure for stiff fluid shell ($\beta = 0$)								
Q_c	a_c	m_c	L_{ic}	L_{ec}	IR	ER	St	Fig
0.4	1.041184	0.631676	-	-	FR	B	BH	1
0.5	1.026782	0.702327	-	-	FR	B	BH	2
2.5	0.937496	10.33415	-	-	FR	B	BH	3
0.4	1.041184	0.422023	2.944657	-	DS	B	GS	4
0.5	1.026782	0.435288	2.574298	-	DS	B	GS	5
2.5	0.937496	10.33415	3.8117×10^7	-	DS	B	GS	6
0.4	1.041184	0.549544	2.944657	2.793761	DS	BDS	GS	7
0.5	1.026782	0.572372	2.574298	2.357312	DS	BDS	GS	8
2.5	0.937496	10.33415	3.8117×10^7	1.67201×10^7	DS	BDS	GS	9

an output of the collapse of a star as shown in Figure 1. We have the similar behavior of potential function for different values of charge (Figures 1-3). Hence, this case gives unstable stable structure under small perturbation for every choice of the physical parameters.

Case (ii): $m \neq 0 \neq Q$, $\Lambda_i \neq 0$ and $\Lambda_e = 0$

This case represents the internal DS region with external Bardeen BH. The corresponding critical values of physical parameters are given in Table 1. In this case, we observe the effects of mass and L_i on the final configuration of the developed structure as shown in Figures 4-6. This case represents the possibility of the existence of bounded excursion gravastar for a suitable choice of physical parameters. It is found that the star shows collapsing behavior for critical values of the physical parameters as given in Table 1. The potential function has four real roots for specific choices of m and L_i with $0 < a_1 < a_2 < a_3 < a_4$. If $a < a_1$, then the potential function approaches to $-\infty$ as $a \rightarrow 0$ that represents the flat spacetime. If $a_1 < a < a_2$, then $V(a) > 0$ which is unstable under small perturbation. If $a_2 < a < a_3$, then $V(a) < 0$ implying the existence of stable bounded excursion gravastar.

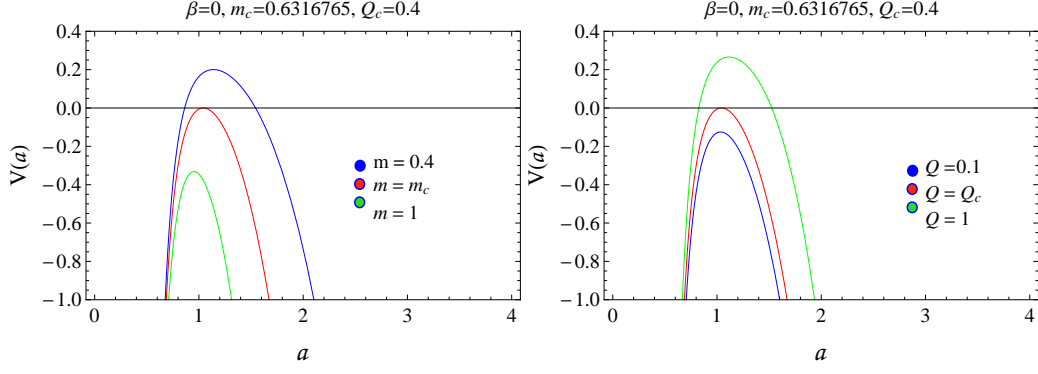


Figure 1: The potential function for interior flat and exterior Bardeen BH with different values of mass (left plot) and charge (right plot).

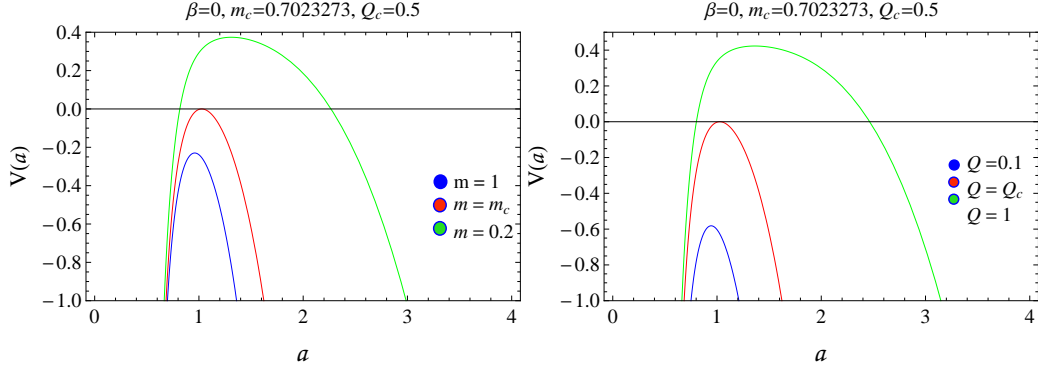


Figure 2: The potential function for interior flat and exterior Bardeen BH with different values of mass (left plot) and charge (right plot).

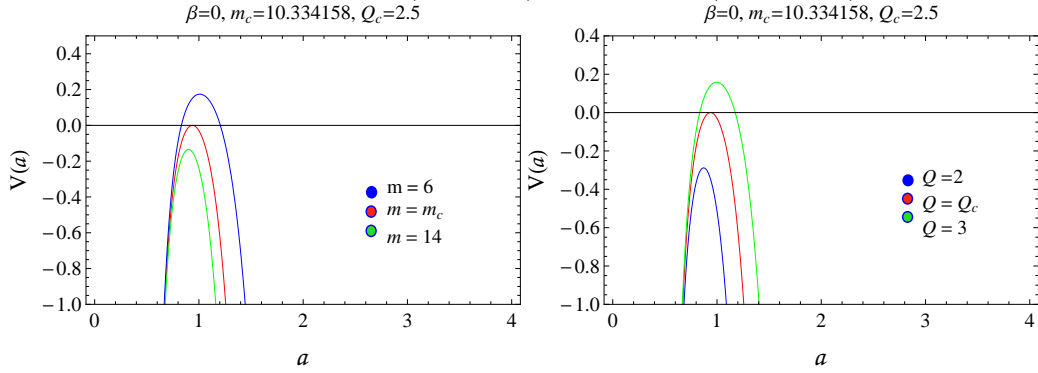


Figure 3: The potential function for interior flat and exterior Bardeen BH with different values of mass (left plot) and charge (right plot).

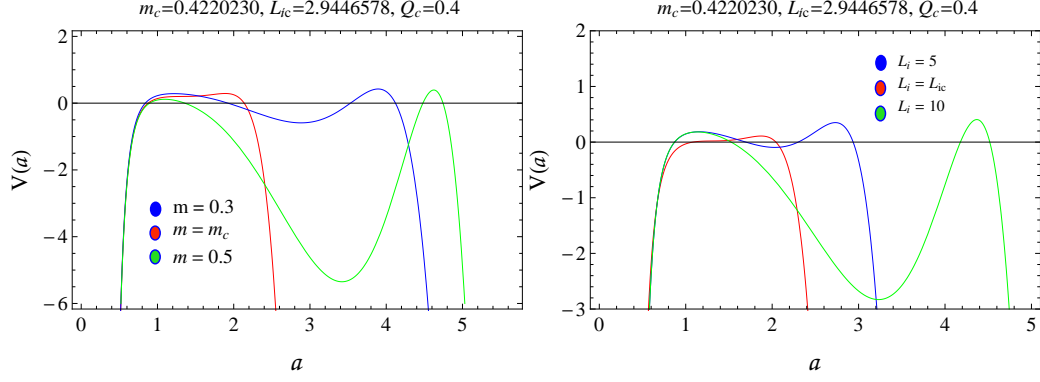


Figure 4: The potential function for interior DS spacetime and exterior Bardeen BH with different values of mass (left plot) and L_i (right plot).

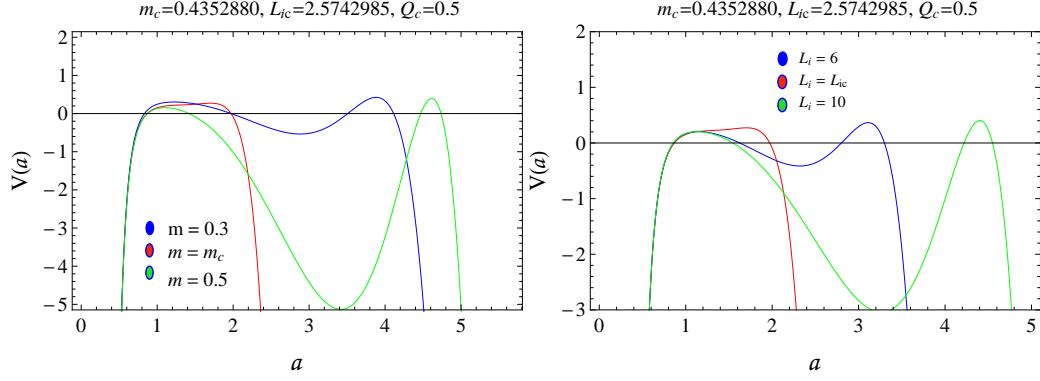


Figure 5: The potential function for interior DS spacetime and exterior Bardeen BH with different values of mass (left plot) and L_i (right plot).

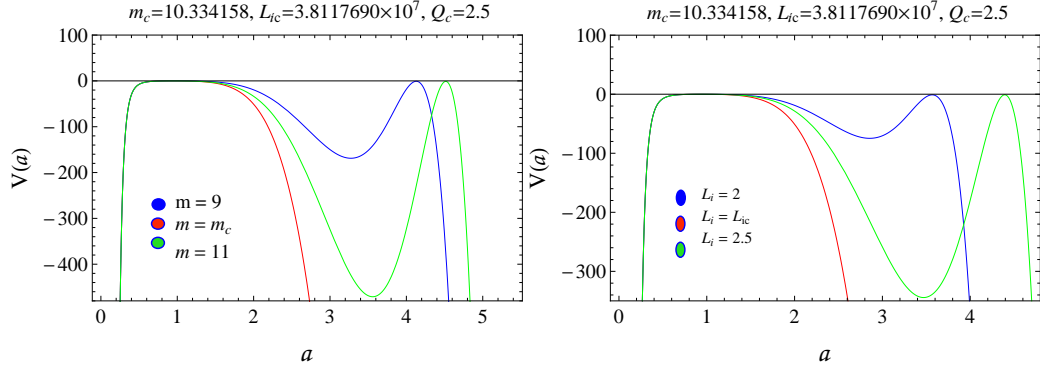


Figure 6: The potential function for interior DS spacetime and exterior Bardeen BH with different values of mass (left plot) and L_i (right plot).

If $a_3 < a < a_4$, then again $V(a) > 0$ which shows unstable configuration under small perturbation. The potential function again approaches to $-\infty$ as $a \rightarrow \infty$ for $a > a_4$ which leads to the formation of BH (Figures 4-6). It is found that the region of the existence of gravastar is very small as compared to the BHs. Hence, the dynamical model cannot completely exclude the possibility of formation of gravastar and BH structure. If the gravastar model exists then there is also a possibility for the existence of BH and vice versa. It is also interesting to mention here that the regions of stable bounded excursion gravastar is enhanced by increasing mass and L_i .

Case (iii): $m \neq 0 \neq Q$ and $\Lambda_i \neq 0 \neq \Lambda_e$

This is the general case which leads to the internal DS region and external Bardeen-DS BH. The critical values of physical parameters are given in Table 1. To avoid the presence of an event horizon in the developed structure, it is found that $\Lambda_i > \Lambda_e$ which corresponds to $L_e > L_i$. It is observed that the obtained critical values of L_i and L_e do not satisfy the required inequality ($L_e > L_i$). Hence, the behavior of stars must be collapsing for these choices of physical parameters. The graphical behavior of potential function shows that the developed structure represents collapse leading to BH if $L_e < L_i$ (Figures 7-9). Therefore, we assume the particular choice of L_i and L_e with $L_e > L_i$ for different values of L_e and Q . It is found that the developed structure shows the existence of stable bounded excursion gravastar if $L_e > L_i$. The regions of stable bounded excursion gravastar increase by increasing L_e and Q .

3.2 Dust Fluid Shell

Here, we explore the results in the presence of dust fluid distribution at the shell. The corresponding expressions of the potential function and its derivative can be written as

$$\begin{aligned}
V(a) &= \frac{1}{2} + \frac{a^6}{4L_e^2 L_i^2} - \frac{a^6}{8L_e^4} - \frac{a^6}{8L_i^4} - \frac{a^2}{4L_e^2} - \frac{a^2}{4L_i^2} - \frac{a^2 m}{2(a^2 + Q^2)^{3/2}} - \frac{1}{8a^2} \\
&\quad - \frac{a^6 m}{2(a^2 + Q^2)^{3/2} L_e^2} + \frac{a^6 m}{2(a^2 + Q^2)^{3/2} L_i^2} - \frac{a^6 m^2}{2(a^2 + Q^2)^3}, \quad (26) \\
V'(a) &= \frac{3a^5}{2L_e^2 L_i^2} - \frac{3a^5}{4L_e^4} - \frac{3a^5}{4L_i^4} + \frac{1}{4a^3} - \frac{am}{(a^2 + Q^2)^{3/2}} + \frac{3a^7 m}{2(a^2 + Q^2)^{5/2} L_e^2}
\end{aligned}$$

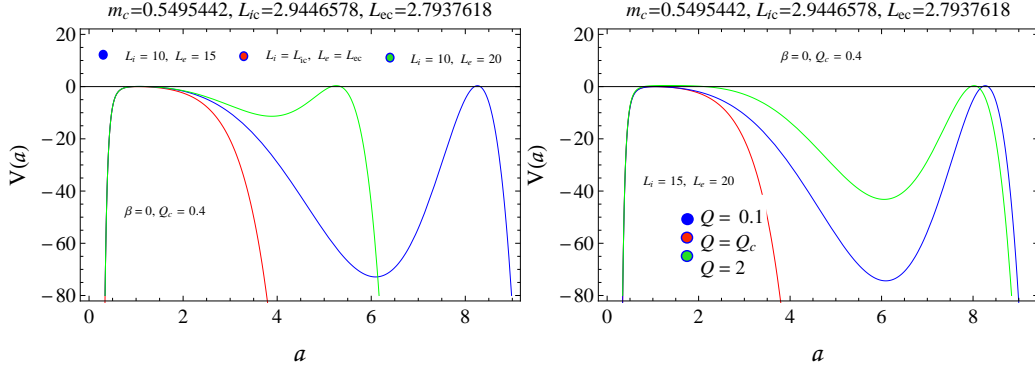


Figure 7: The potential function for interior DS spacetime and exterior Bardeen-DS BH with different values of L_i , L_e (left plot) and charge (right plot).

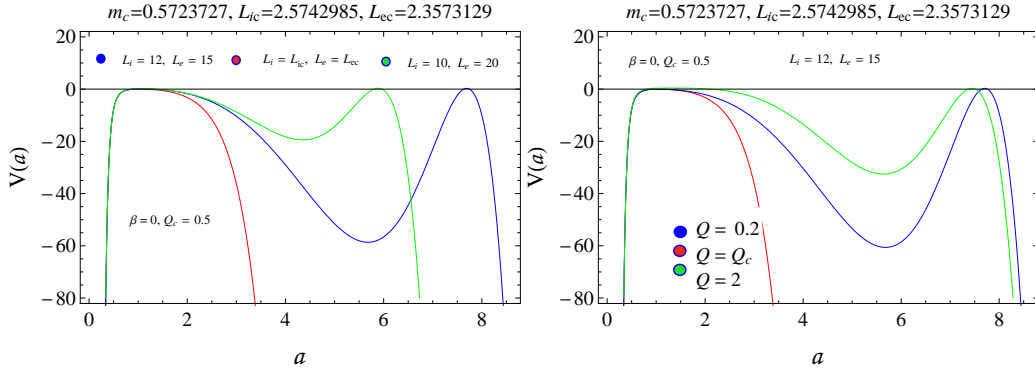


Figure 8: The potential function for interior DS spacetime and exterior Bardeen-DS BH with different values of L_i , L_e (left plot) and charge (right plot).

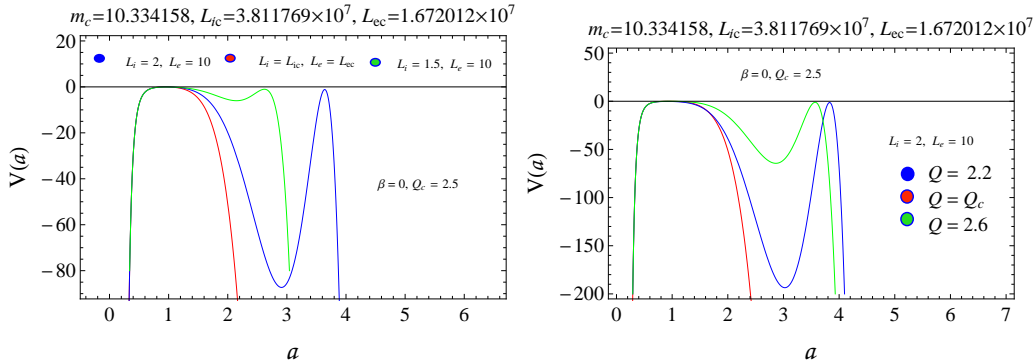


Figure 9: The potential function for interior DS spacetime and exterior Bardeen-DS BH with different values of L_i , L_e (left plot) and charge (right plot).

Table 2: Critical values of physical parameters and outcomes of the developed structure for dust fluid shell with different internal and external geometries.

Final outcomes of developed structure for dust fluid shell ($\beta = 1$)								
Q_c	a_c	m_c	L_{ic}	L_{ec}	IR	ER	St	Fig
0.7	1.918218	0.891839	-	-	FR	B	NS	10
0.8	2.981319	0.923782	-	-	FR	B	NS	11
1.5	0.703307	3.778338	-	-	FR	B	BH	12
0.7	1.021781	0.909516	6.64462×10^7	-	DS	B	GS	13
0.8	2.981319	1.636369	15.37334	-	DS	B	GS	14
1.5	12.79669	0.980800	4.15909×10^9	-	DS	B	GS	15
0.7	1.918218	0.880891	8.692764	10.64767	DS	BDS	GS	16
0.8	2.981319	0.916398	15.37334	17.40656	DS	BDS	GS	17
1.5	12.79669	0.978446	109.3384	112.3030	DS	BDS	GS	18

$$\begin{aligned}
& - \frac{3a^7 m}{2(a^2 + Q^2)^{5/2} L_i^2} + \frac{3a^7 m^2}{(a^2 + Q^2)^4} - \frac{3a^5 m}{(a^2 + Q^2)^{3/2} L_e^2} - \frac{3a^5 m^2}{(a^2 + Q^2)^3} \\
& + \frac{3a^5 m}{(a^2 + Q^2)^{3/2} L_i^2} + \frac{3a^3 m}{2(a^2 + Q^2)^{5/2}} - \frac{a}{2L_e^2} - \frac{a}{2L_i^2}, \quad (27)
\end{aligned}$$

respectively. The respective critical values for different choices of interior and exterior regions are expressed in Table 2. We choose suitable values of charge for which the system shows real critical values of physical parameters.

Case (i): $m \neq 0 \neq Q$ and $\Lambda_i = 0 = \Lambda_e$

The results of the collapse of a shell with internal flat and external Bardeen BH are shown in Figures 10-12. The potential function represents the stable configuration of the developed structure for every value of mass and charge which denotes the presence of normal star (Figures 10 and 11). The shell shows collapsing behavior ($V(a) < 0$) for small values of shell radius and then shows expansion ($V(a) > 0$). Figure 12 indicates the collapsing configuration which leads to the formation of BHs. There is no possible way to develop gravastar for every choice of physical parameters.

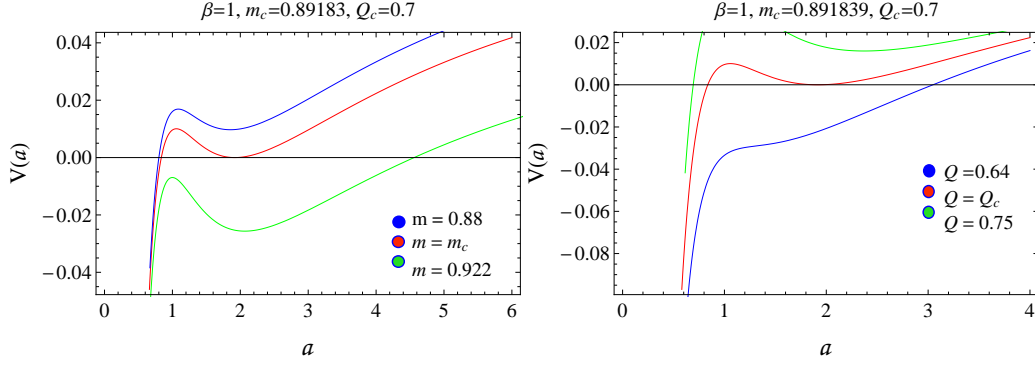


Figure 10: The potential function for interior flat and exterior Bardeen BH with different values of mass (left plot) and charge (right plot).

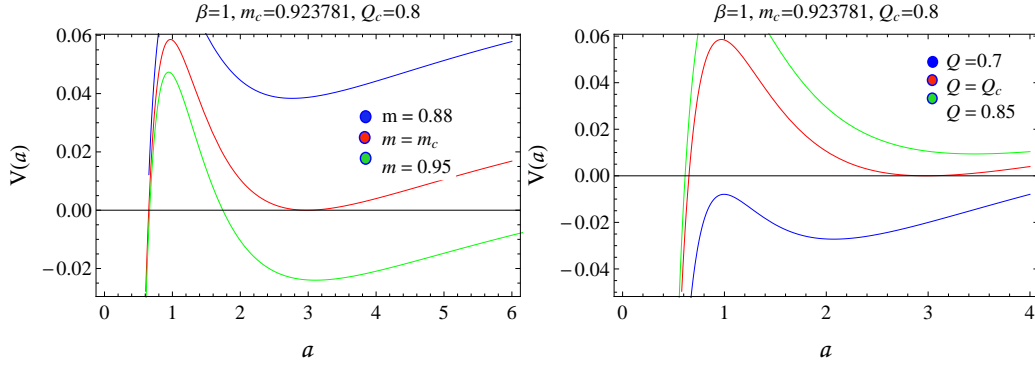


Figure 11: The potential function for interior flat and exterior Bardeen BH with different values of mass (left plot) and charge (right plot).

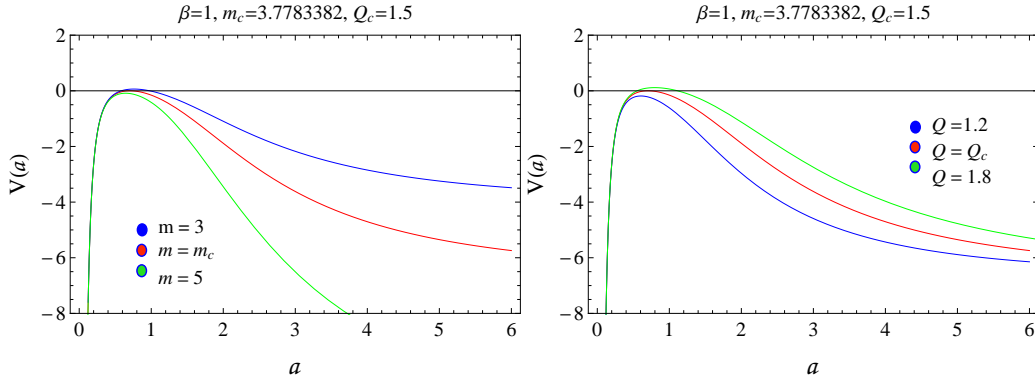


Figure 12: The potential function for interior flat and exterior Bardeen BH with different values of mass (left plot) and charge (right plot).

Case (ii): $m \neq 0 \neq Q$, $\Lambda_i \neq 0$ and $\Lambda_e = 0$

Here we take the collapse of internal DS and external Bardeen BH through critical values given in Table 2. This is the most suitable case for the existence of stable bounded excursion gravastar. The stable gravastar must exist for the choice of considered critical values (Table 2) as shown in Figures 13-15. The potential function has two real roots as $0 < a_1 < a_2$. If $a < a_1$, then the potential function approaches to $-\infty$ as $a \rightarrow 0$ that represents the flat spacetime. If $a_1 < a < a_2$, then the potential function is less than zero and hence expresses the existence of stable bounded excursion gravastar. If $a_2 < a$, then $V(a)$ approaches to plus or minus infinity that express the expansion and collapsing behavior as $a \rightarrow \infty$. It is found that the choice of Bardeen BH as an exterior geometry of shell filled with dust fluid provides stable bounded excursion gravastar as compared to the choice of Schwarzschild/Schwarzschild DS/RN geometries [11, 13, 14]. Hence, this is more suitable for the construction of stable gravastar with a dust shell.

Case (iii): $m \neq 0 \neq Q$ and $\Lambda_i \neq 0 \neq \Lambda_e$

We consider the internal DS region and external Bardeen DS BH. The critical values (Table 2) follow the inequality $L_e > L_i$ with every considered choice of Q . Hence, the developed structure is suitable to eliminate the presence of an event horizon and singularity for critical values. The graphical behavior of potential function shows the expanding behavior which gives information about the existence of stable gravastar near the suitable critical values of physical parameters (Figures 16-18). Hence, the stable gravastar must exist for the different choices of m and Q .

4 Final Remarks

This work is the extension of stability issues related to the possible existence of stable bounded excursion gravastar from a model consisting of internal DS region, intermediate thin-shell filled with matter distribution followed the EoS $p = (1 - \beta)\rho$ and external Schwarzschild DS as well as RN spacetimes [11, 13, 14]. Here, we are interested to explore the existence of bounded excursion gravastar in the background of exterior regular Bardeen and Bardeen DS BHs. We have used cut and paste approach to match these spacetimes at the shell. The potential function of the shell filled with matter distribution

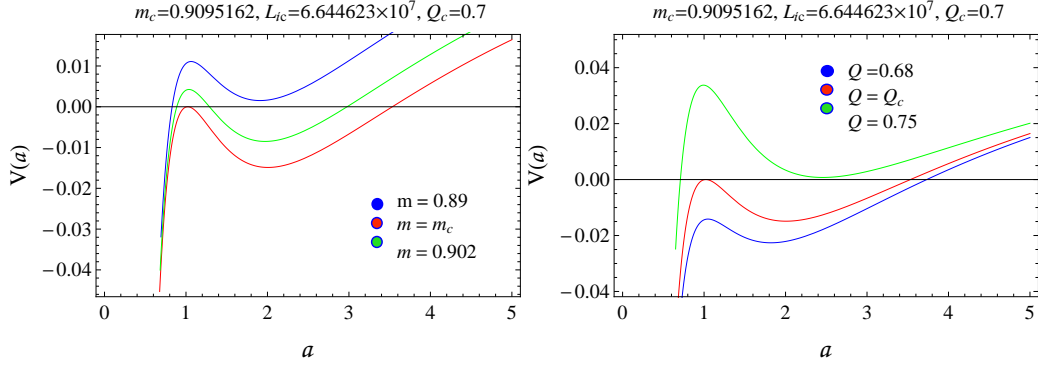


Figure 13: The potential function for interior DS spacetime and exterior Bardeen BH with different values of mass (left plot) and charge (right plot).

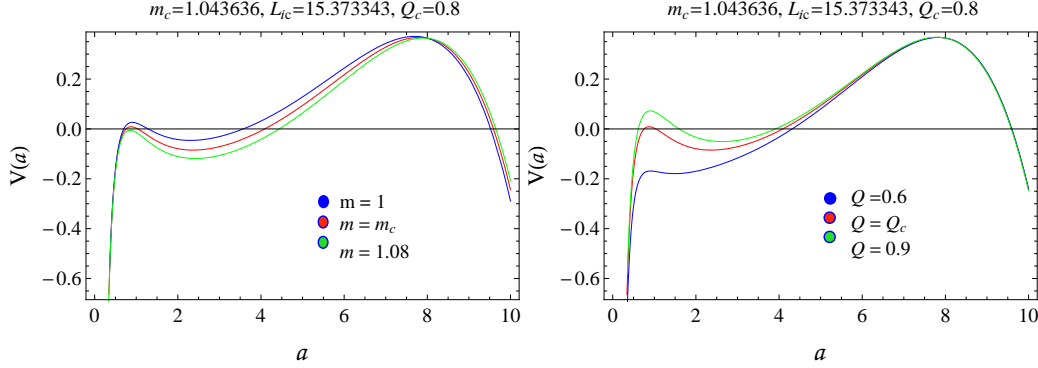


Figure 14: The potential function for interior DS spacetime and exterior Bardeen BH with different values of mass (left plot) and charge (right plot).

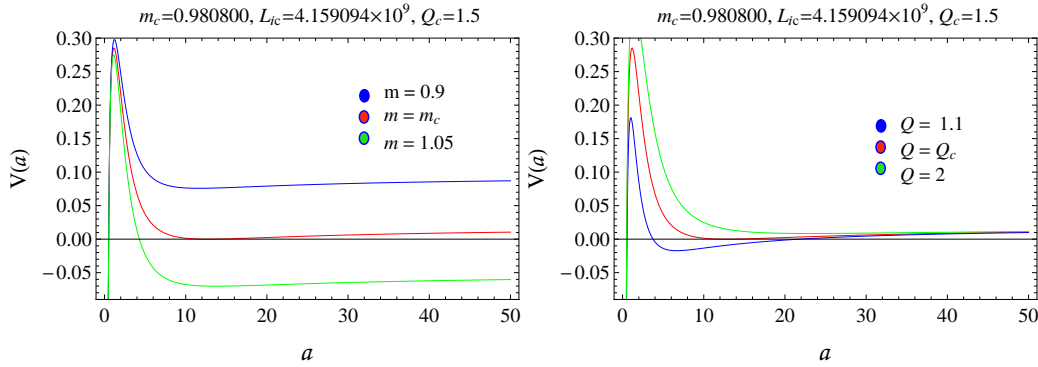


Figure 15: The potential function for interior DS spacetime and exterior Bardeen BH with different values of mass (left plot) and charge (right plot).

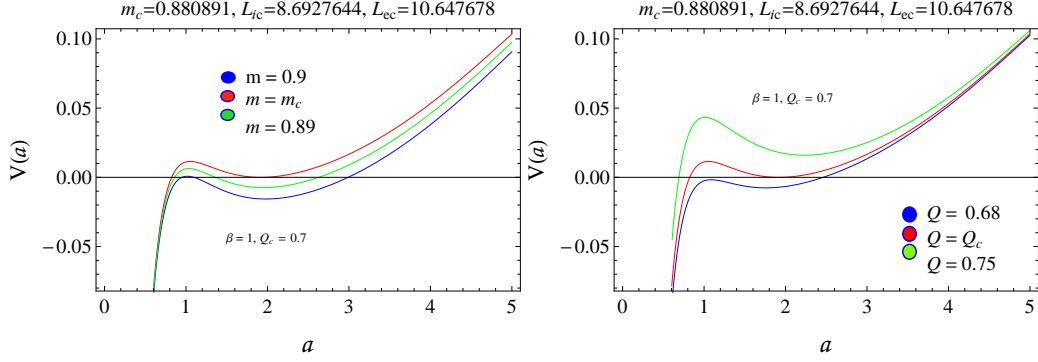


Figure 16: The potential function for interior DS spacetime and exterior Bardeen DS BH with different values of mass (left plot) and charge (right plot).

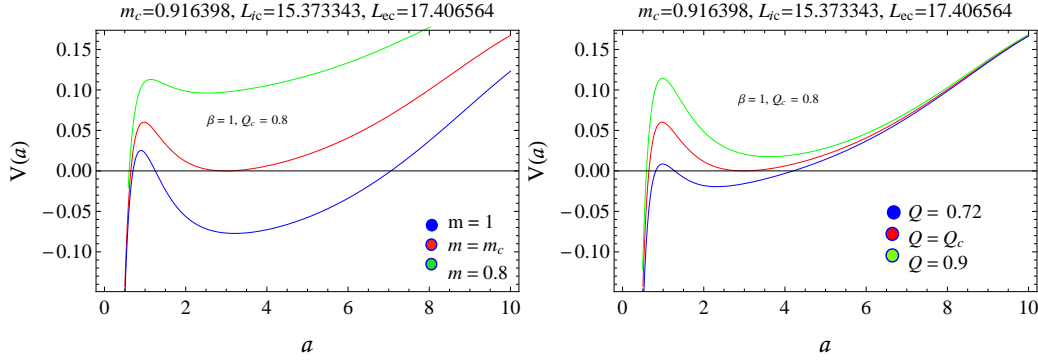


Figure 17: The potential function for interior DS spacetime and exterior Bardeen DS BH with different values of mass (left plot) and charge (right plot).

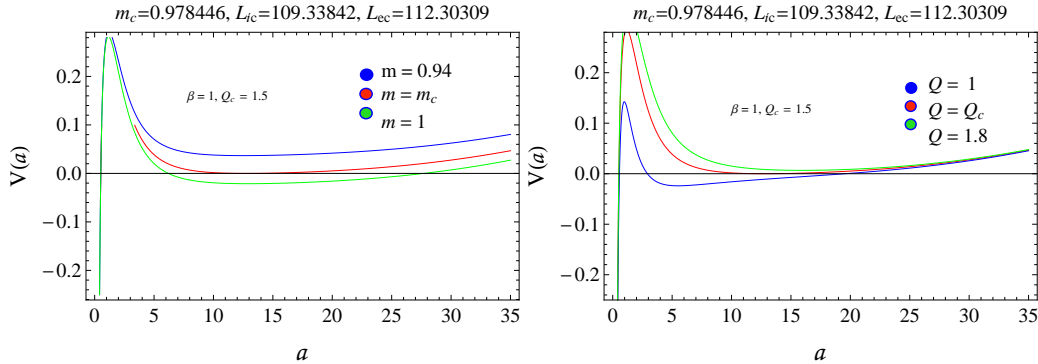


Figure 18: The potential function for interior DS spacetime and exterior Bardeen DS BH with different values of mass (left plot) and charge (right plot).

($p = (1 - \beta)\rho$) can be evaluated through the equation of motion of shell. The developed framework is investigated through the critical values of physical parameters by solving the following equations $V(a) = 0$ and $V'(a) = 0$, simultaneously. For this purpose, we have considered two types of matter distribution stiff ($\beta = 0$) and dust ($\beta = 1$) fluids.

For the stiff fluid shell, the critical values of physical parameters for three different cases are given in Table 1. For the interior flat spacetime and exterior Bardeen BHs, we have obtained the collapsing behavior of the shell which indicates the formation of BHs (Figures 1-3). The interior DS and exterior Bardeen BH represent the region of stable bounded excursion gravastar for a suitable choice of physical parameters. If the gravastar model exists then there is a possibility for the existence of BH and vice versa. We have analyzed that the regions of stable bounded excursion gravastar increase by increasing mass and L_i (Figures 4-6). For the interior DS and exterior Bardeen DS BH, we have obtained that bounded excursion stable gravastar must exist if $L_i < L_e$ (Figures 7-9). The regions of bounded excursion gravastar increase by enhancing charge and L_e .

For dust fluid shell, we have obtained the respective critical values of physical parameters (Table 2). There does not exist the possibility of the existence of gravastar for the flat and exterior Bardeen BH (Figures 10-12). The stable structure of bounded excursion gravastar is found for every choice of physical parameters for interior DS and exterior Bardeen BH (Figures 13-15). The stable bounded excursion gravastar is determined for suitable choices of physical parameters with interior DS and exterior Bardeen DS BH (Figures 16-18).

We conclude that the gravastar model in the background of regular BHs is more feasible for the existence of a stable configuration of bounded excursion gravastar than the Schwarzschild and RN BHs [11, 13, 14]. These BHs do not provide any region of stable gravastar for the choice of dust shell while our models show stable regions of bounded excursion gravastar. This paper also follows the previous results for the choice of $Q = 0$ [13].

References

- [1] Wald, R.M.: Living Rev. Real. 4(2001)6.
- [2] Mazur, P. and Mottola, E.: arXiv: gr-qc/0109035.

- [3] Mazur, P. and Mottola, E.: Proc. Nat. Acad. Sci. **101**(2004)9545.
- [4] Chapline, G., Hohlfeld, E., Laughlin, R.B. and Santiago, D.I.: Int. J. Mod. Phys. A **18**(2003)3587.
- [5] Vachaspati, T.: 2007 Preprint0706.1203
- [6] Copeland, E.J., Sami, M. and Tsujikawa, S.: Int. J. Mod. Phys. D **15**(2006)1753.
- [7] Visser, M. and Wiltshire, D.L.: Class. Quantum Grav. **21**(2004)1135.
- [8] Carter, B.M.N.: Class. Quantum Grav. **22**(2005)4551.
- [9] Horvat, D., Sasa Ilijic, S. and Marunovic, A.: Class. Quantum Grav. **26**(2009)025003.
- [10] Rahaman, F., Usmani, A.A., Ray, S. and Islam, S.: Phys. Lett. B **707**(2012)319; *ibid.* **717**(2012)1.
- [11] Rocha, P., et al.: J. Cosmol. Astropart. Phys. **06**(2008)25; *ibid* **11**(2008)010.
- [12] Chan, R., da Silva, M.F.A., Rocha, P., and Wang, A.: J. Cosmol. Astropart. Phys. **03**(2009)10.
- [13] Chan, R., da Silva, M.F.A. and Rocha, P.: J. Cosmol. Astropart. Phys. **12**(2009)17.
- [14] Chan, R. and da Silva, M.F.A.: J. Cosmol. Astropart. Phys. **07**(2010)29.
- [15] Lobo, F.S.N. and Garattini, R.: J. High Energy Phys. **1312**(2013)065.
- [16] Övgün, A., Banerjee, A. and Jusufi, K.: Eur. Phys. J. C **77**(2017)566.
- [17] Sharif, M. and Javed, F.: Ann. Phys. **415**(2020)168124.
- [18] Lobo, F.S.N.: Class. Quantum Grav. **23**(2006)1525.
- [19] DeBenedictis, A., et al.: J. Cosmol. Astropart. Phys. **23**(2006)2303.
- [20] Horvat, D. and Ilijić, S.: J. Cosmol. Astropart. Phys. **24**(2007)5637.

- [21] Chan, R., da Silva, M.F.A. and Rocha, P.: Gen. Relativ. Gravit. **43**(2011)2223.
- [22] Horvat, D., Ilijic, S. and Marunovic, A.: Class. Quantum Grav. **28**(2011)195008.
- [23] Chan, R., et al.: J. Cosmol. Astropart. Phys. **10**(2011)013.
- [24] Banerjee, A., Rahaman, F., Islam, S. and Govender, M.: Eur. Phys. J. C **76**(2016)34.
- [25] Ghosh, S., Rahaman, F., Guha, B.K. and Ray, S.: Phys. Lett. B **767**(2017)380.
- [26] Shamir, M.F. and Ahmad, M.: Phys. Rev. D **97**(2018)104031.
- [27] Yousaf, Z., et al.: Phys. Rev. D **100**(2019)024062.
- [28] Sharif, M. and Waseem, A.: Astrophys. Space Sci. **364**(2019)189.
- [29] Sharif, M. and Javed, F.: Chin. J. Phys. **61**(2019)262; Astrophys Space. Sci. **364**(2019)179; Int. J. Mod. Phys. A **35**(2020)2040015; Int. J. Mod. Phys. D **29**(2020)2050007.
- [30] Bardeen, J.M.: Proceedings of GR5 (Tiflis, USSR, 1968)174.
- [31] Ayón-Beato, E. and García, A.: Phys. Rev. Lett. **80**(1998)5056; Bronnikov, K.A.: Phys. Rev. Lett. **85**(2000)4641; Phys. Rev. D **63**(2001)044005; Hayward, S.A.: Phys. Rev. Lett. **96**(2006)031103.
- [32] Fernando, S.: Int. J. Mod. Phys. D **26**(2017)1750071.
- [33] Singh, D.V. and Singh, N.K.: Ann. Phys. **383**(2017)600.
- [34] Ali, M.S. and Ghosh, S.G.: Phys. Rev. D **98**(2018)084025.
- [35] Dey, S. and Chakrabarti, S.: Eur. Phys. J. C **79**(2019)504.
- [36] Sharif, M. and Javed, F.: Astrophys Space. Sci. **364**(2019)179.
- [37] Alshal, H.: Europhys. Lett. **128**(2019)60007.
- [38] Li, C., et al.: Mod. Phys. Lett. A **34**(2019)1950336.

- [39] Perlmutter, S. et al.: *Astrophys. J.* **517**(1999)565; Riess, A.G. et al.: *Astron. J.* **117**(1999)707; *ibid* *Astron. J.* **116**(1998)1009; Spergel, D.N. et al.: *Astrophys. J. Suppl.* **170**(2007)377.
- [40] Lake, K.: *Phys. Rev. D* **19**(1979)2847.